Acta Cryst. (1994). A**50**, 239–246

Experimental Verification of the Statistical Dynamical Theories of Diffraction

BY TOSHIHIKO TAKAMA AND HIDEKI HARIMA*

Department of Applied Physics, Faculty of Engineering, Hokkaido University, Kita-ku, Sapporo 060, *Japan*

(*Received* 27 *May* 1993; *accepted* 17 *September* 1993)

Abstract

The influences of crystal imperfection on dynamical diffraction have been studied by measuring integrated intensities in the Laue case as a function of X-ray wavelength. SiO_2-precipitate microdefects were introduced into Czochralski-grown silicon wafers by heating at 1223 K for five different periods of time varying from 25 to 145 h. The X-ray intensities were measured by the energy-dispersive diffraction method over the wavelength range 0.15 to 0.78 Å. The measurements revealed that increases in both the integrated intensity and the *Pendellösung* beat spacing were accompanied by a decrease of the beat amplitude with increasing heating period. The data were compared quantitatively with those obtained using the theories of Kato [*Acta Cryst.* (1980), A**36**, 763–769, 770–778] and Becker & Al Haddad [*Acta Cryst.* (1992), A**48**, 121–134). The former theory, where the correlation length Γ for the wavefield amplitudes is assumed to be close to the extinction distance, did not describe the data. The latter theory fitted only the specimen heated for 25 h. A model assuming that Γ is independent of wavelength and varies with crystal perfection and reflection plane was proposed in lieu of Kato's assumption. The application of the model led to an excellent agreement for the specimens studied. The best fitted values of Γ, from 0.07 to 1.6 μm, were much the same as the correlation lengths of the phase factor, from 0.04 to 2.6 μm.

1. Introduction

The most widely adopted approach to the secondary extinction correction is based on the idea of mosaic blocks introduced by Darwin (1922). It assumes that the waves in the block propagate coherently but no waves diffracted from different blocks interfere. Later, Hamilton (1957) and Zachariasen (1967) took over the idea and proposed energy-transfer equations to describe the coupling between the transmitted and diffracted beams. The treatment has been successful in practical applications to the extinction correction. The idea is doubtful, however, since real crystals are not composed of such ideal blocks.

In contrast, Takagi (1962) and Taupin (1964) (Takagi–Taupin) proposed amplitude-transfer equations to describe the wavefields in imperfect crystals. The nature of the imperfection caused by lattice displacement $\mathbf{u}(\mathbf{r})$ is taken into the equations through the phase factor $\exp(2\pi i\mathbf{g}\mathbf{u})$ for the $\mathbf{g}$ reflection. In real crystals, the essential property of the lattice distortion is in the statistical distribution. On this basis, Kato (1980*a*,*b*) succeeded in developing the statistical dynamical theory. There, the distribution of the distortion is considered as a statistical object. The theory is expressed in terms of three parameters. One is just the static Debye–Waller factor E; the others are the correlation lengths of the phase factor τ and the wavefield Γ. The theory is free from the traditional treatment involving the idea of mosaic blocks.

Some effort has been made to test and improve the theory. Olekhnovich, Karpei, Olekhnovich & Puzenkova (1983) measured the integrated intensity of X-rays as a function of crystal thickness for a series of silicon wafers with dislocations. They observed an expansion of the *Pendellösung* fringe spacing and an attenuation of the oscillations at low dislocation density. The results were analyzed by an approach based on Kato's theory. They concluded that this approach was not suitable for describing their data. Later, the minor mistakes in Kato's theory were indicated by Al Haddad & Becker (1988) and Guigay (1989) independently. Al Haddad & Becker re-analyzed the same data and showed their good agreement with the modified theory.

Recently, Becker & Al Haddad (1990, 1992) have come to suspect Kato's assumption that Γ is of the same magnitude as the extinction distance. According to them, Γ fluctuates around the correlation length τ. The difference in Γ has a definite influence on the diffuse scattering. The experimental test for the two theories was performed by comparing the results with those of γ-ray diffraction by Schneider, Bouchard, Graf & Nagasawa (1992). These authors measured the thickness dependence of the integrated diffracting power for heat-treated Czochralski-grown silicon. The test showed that the approach used by Becker & Al Haddad excellently describes their data and that Kato's assumption must be abandoned. Recently, Kato (1991) has developed a more rigorous theory; however, it is still in the development stage and its practical application to diffraction has not

* Present address: Image and Measurement Division, Nippon Steel Co. Ltd, Fuchinobe, Sagamihara 229, Kanagawa, Japan.

ISSN 0108-7673

yet been concretely shown. Therefore, we deal only with the old theory (Kato, 1980*a*,*b*) in the present study.

The statistical dynamical theory is expected to cover the full range of diffraction from imperfect to perfect crystals. Therefore, it is desirable to employ an experimental method that allows one to investigate the characteristic diffraction from imperfect and perfect crystals. *Pendellösung* fringes are a good example for dynamical diffraction. In most studies, these fringes have been observed as a function of crystal thickness. We have proposed an experimental technique (Takama, Iwasaki & Sato, 1980; Takama & Sato, 1988) for measuring the *Pendellösung* beats as a function of X-ray wavelength. It is an effective method of testing Kato's assumption that Γ varies with wavelength. The purpose of the present work is to investigate the integrated intensity from silicon samples with different distorted states and to verify the statistical dynamical theories.

2. Brief outline of the statistical dynamical theories

Kato's theory starts with the ensemble average of the Takagi–Taupin equations for the amplitudes of the transmitted and the diffracted waves as well as the lattice phase factor φ. The factor φ at a position $\mathbf{r}$ is expressed by the sum of the average and the deviation as

$$\varphi(\mathbf{r}) = \exp(2\pi i \mathbf{g}\mathbf{u}) = \langle\varphi\rangle + \delta\varphi(\mathbf{r}) = E + \delta\varphi(\mathbf{r}). \quad (1)$$

Here, $\mathbf{g}$ and $\mathbf{u}$ are the reciprocal-lattice vector and the displacement of the lattice, respectively. The quantity E is the so-called static Debye–Waller factor. Kato introduced the two correlation lengths τ and Γ. The correlation length of the phase factor τ is defined by

$$\tau = \int_0^\infty \langle\delta\varphi(0)\delta\varphi^*(z)\rangle(1 - E^2)^{-1}\,\mathrm{d}z. \quad (2)$$

The length τ is the distance above which the phase correlation is lost. The expression for the correlation length Γ of the wavefield amplitudes is not given directly from its definition. Kato expected Γ to be of the functional form $\Gamma = \Lambda_g/E$. The proposed Γ is inversely proportional to the wavelength λ through the extinction distance $\Lambda_g = v/(\lambda C r_e F_g)$. Here, v is the volume of the unit cell and the polarization factor C is equal to unity for the σ mode and to $|\cos 2\theta|$ for the π mode of X-ray polarization. The quantities r_e and F_g denote the radius of the classical electron and the structure factor of the g reflection, respectively. The correlation between φ and wavefields is ignored and an isotropic medium is assumed. Kato (1980*b*) gave analytical expressions for the integrated intensity using the three parameters. It consists of four components: coherent, R^C; incoherent, R^I; mixed, R^M and Borrmann absorption, R^B.

Becker & Al Haddad (1992) derived new propagation equations to describe the diffuse scattering. With certain assumptions, they showed that Γ fluctuates around τ. It should be noticed that, even though Γ in Kato's theory is simply replaced with τ_2,† the resultant intensities for the incoherent and the mixed components are not identical to Kato's predictions.

The integrated intensity (total diffracted power) J of a Laue spot for the symmetrical Laue case is given by

$$J = K(\lambda)(R_\sigma + |\cos 2\theta| R_\pi)/2 = K(\lambda)R. \quad (3)$$

if the incident beam is unpolarized (Buras & Gerward, 1975), where R_j ($j = \sigma$ and π) stands for the sum of the four terms R_j^C, R_j^I, R_j^M and R_j^B for the j mode of the polarization. The term $K(\lambda)$ is a monotonously varying function given by

$$K(\lambda) = AF_g i_0(\lambda)\exp[-\mu(\lambda)t/\cos\theta]\lambda, \quad (4)$$

with the λ-independent term $A = Sr_e/(v|\mathbf{g}|^2)$, where $i_0(\lambda)$ represents the incident-beam intensity, $\mu(\lambda)$ the linear absorption coefficient, t the crystal thickness, θ the Bragg angle at λ and S the cross section of the incident beam.

The two theories provide the same equation for the coherent component:

$$R_j^C = EW[2ET/\Lambda_g]\exp[-2(1 - E^2)T\tau/\Lambda_g^2] \quad (5)$$

with $T = t/\cos\theta$. The Waller integral $W[2x] = \int_0^{2x} J_0(\rho)\,\mathrm{d}\rho$ gives rise to the *Pendellösung* beat with respect to t and λ in the upper limit $2x = 2ET/\Lambda_g$. The integrand J_0 denotes the Bessel function of the zeroth order of the first kind. In comparison with the perfect crystal with $E = 1$, the *Pendellösung* spacing is increased by a factor of $1/E$ owing to the modification of the upper limit.

There are remarkable differences in the incoherent R_j^I and the mixed components R_j^M between the two theories. R_j^I according to Kato (Ka) is

$$R_j^I(\mathrm{Ka}) = (1 - E^2)/\tau_{\mathrm{Ka}}\sinh(2\tau_{\mathrm{Ka}}T_{\mathrm{eff}}) \times \exp(-2\tau_{\mathrm{Ka}}T_{\mathrm{eff}}), \quad (6a)$$

where $\tau_{\mathrm{Ka}} = [E^2\Gamma + (1 - E^2)\tau]/\Lambda_g$ and $T_{\mathrm{eff}} = T/\Lambda_g$. R_j^I according to Becker & Al Haddad (BA) is more complicated and is given by

$$R_j^I(\mathrm{BA}) = (1 - E^2)\exp(-2U)\{\sinh(2U)/\tau_{\mathrm{BA}} + [\tau_x/(\tau_{\mathrm{BA}}^2 - \tau_x^2)][\exp(-2\tau_x T_{\mathrm{eff}}) + (\tau_x/\tau_{\mathrm{BA}})\sinh(2U) - \cosh(2U)]\}, \quad (6b)$$

where $\tau_{\mathrm{BA}} = (1 - E^2)\tau_2/\Lambda_g$, $U = \tau_{\mathrm{BA}}T_{\mathrm{eff}}$ and $\tau_x = E^2\tau/\Lambda_g$.

† Hereinafter, the symbol τ_2 is used for Γ in representations of the theory of Becker & Al Haddad.

The equations for R_j^M are even more complicated. For the exact expressions, the reader may refer to the papers by Kato (1980*b*), Guigay (1989) and Becker & Al Haddad (1992).

For a perfect crystal with $E = 1$, both R_j^I and R_j^M vanish and the remaining R_j^C and R_j^B provide the intensity predicted by the traditional dynamical theory. In the limit of small correlation lengths, *i.e.* as τ/Λ_g and Γ/Λ_g go to zero, R_j^M according to Kato tends to zero. Neglecting the Borrmann absorption term, one gets the asymptotic expression from (5) and (6*a*):

$$R_j \simeq EW[2ET/\Lambda_g] + 2(1 - E^2)T/\Lambda_g. \qquad (7)$$

The limit of R_j^M according to Becker & Al Haddad is dependent on the ratio of τ_2 to τ. For $\tau_2 = \tau/2$, it is the same as (7). For $\tau_2 \neq \tau/2$, the additional term P appears from n_3 as defined in equation (78) of Becker & Al Haddad (1992) for R_j^M. The term is approximated by

$$P = (p + 1)/(2p^2)E^2T/\Lambda_g \qquad (8)$$

with $p = (2\tau_2 - \tau)/\tau$. This becomes predominant for p close to zero. The second term in (7) and P of (8) are proportional to t and $\lambda/\cos\theta$ through T/Λ_g.

3. Experimental procedure

Czochralski-grown (CZ) silicon typically contains about 10^{18} O atoms cm^{-3} in the interstitial sites. Since oxygen is supersaturated at lower temperatures, heat treatment leads to oxygen precipitation, which results in the formation of amorphous or crystalline SiO_x ($x \simeq 2$) precipitates. The volume of the precipitate per SiO_2 unit is of roughly twice the atomic volume of silicon in the silicon lattice (Shimura, 1989). Accordingly, the precipitates compress the silicon matrix and produce strain fields. Heat treatment at temperatures above 1173 K leads to softening of the silicon lattice and the strain fields can relax by the emission of dislocation loops and/or stacking faults around the precipitates (Schneider *et al.*, 1992). In the present study, the parallel-sided CZ silicon wafers with [001] surface orientation and 456 (1) μm thickness were subjected to heating in argon gas at 1223 K. The heating time for each specimen is shown in Table 1. The induced defects were assumed to be distributed randomly in the wafers.

The integrated intensities for the symmetrical Laue case were measured with respect to the wavelength of the X-rays at 294 K. White X-rays were produced from a rotating copper anode in a specially designed X-ray generator (Rigaku RU-1000C) operated at 110 kV and 25 mA. The incident beam was collimated by slits of height 0.5 mm and width 0.2 mm for the measurements of the 220 and 440 reflections and by slits of height 0.5 mm and width 0.5 mm for the 400 and 800 reflections. The specimens were mounted on a four-circle goniometer. The diffracted intensities of a Laue spot were counted by a solid-state detector (intrinsic germanium) and the photon energy was analyzed by a multichannel pulse-height analyzer (MCA). The goniometer and MCA were controlled by a microcomputer. The MCA channel widths for collecting the intensities were set in advance in the computer. The integrated intensity J was evaluated after subtraction of the background intensity within the width. The regions of interest were used to calculate the thermal diffuse scattering. The variation of J was obtained by repetition of the same measurement at different Bragg angles. No monitor counter was used to account for the fluctuations in the incident-beam intensity. The fluctuations were estimated by comparing the total intensities of the 220 reflection measured for specimen I prior to, during and after the series of measurements. The total intensities agreed to within ±0.9%. This indicates that the incident-beam intensity was stable.

Table 1. *Heating time for each specimen and mean square displacement* $\langle u^2 \rangle$

Specimens II to VI were heated at 1223 K in argon gas. Numerical values of $\langle u^2 \rangle$ are evaluated from Fig. 5 using (12).

Specimen	Heating time (h)	$\langle u^2 \rangle$ (Å^2)
I	0	-
II	25	0.00062 (14)
III	40	0.0098 (20)
IV	50	0.0160 (19)
V	90	0.0345 (20)
VI	145	0.0449 (14)

4. Experimental results

The integrated intensities were measured for four reflections of six specimens. The profiles of J showed a similar structure for all the reflections. We therefore mainly deal with the 400 reflection as an example. Fig. 1

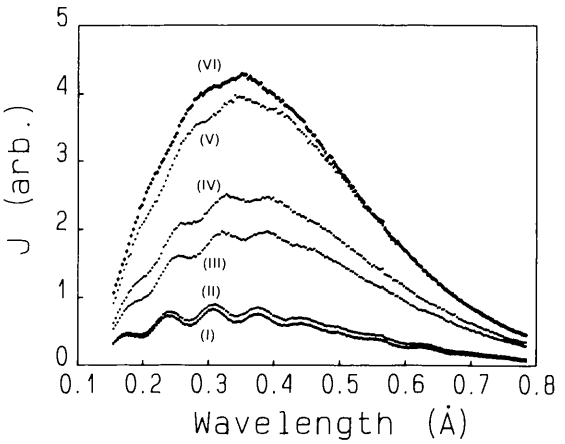

Fig. 1. Integrated intensities J measured for the 400 reflection as a function of X-ray wavelength. Heating times for the specimens: (I) 0 (not heated), (II) 25, (III) 40, (IV) 50, (V) 90 and (VI) 145 h. A fading owing to X-ray polarization is seen near 0.5 Å.

demonstrates a typical example of J. The profiles change remarkably with the heating time. The oscillation in the figure corresponds to the *Pendellösung* beats caused by the change in the extinction distance.

As shown in (3), J contains the term $K(\lambda)$, which is dependent on the wavelength and the reflection plane but independent of crystal perfection. In order to clarify the change in intensity and to simplify the comparison with the theories, the measured J were corrected by a factor $K(\lambda)$. It is necessary to know the precise λ dependence of $\mu(\lambda)$ and $i_0(\lambda)$ in $K(\lambda)$ for the correction; however, it is difficult to measure the λ dependence of $i_0(\lambda)$. Besides, we do not have reliable values of $\mu(\lambda)$. In the course of the present study, $K(\lambda)$ for each reflection was obtained by comparing the J measured for specimen I with that calculated by (3) with $E = 1$. Thermal diffuse scattering $I_{\rm TDS}$ was included in the calculated intensity following the observations of Graf, Schneider, Freund & Lehmann (1981), so that $K(\lambda)$ is estimated by the relation

$$K(\lambda) = J(\lambda)/[R(\lambda) + I_{\rm TDS}(\lambda)]. \qquad (9)$$

The structure factors of silicon measured by Saka & Kato (1986) and the theoretical anomalous-dispersion terms of Sasaki (1989) were adopted for the calculation. The thermal diffuse scattering was evaluated using a program developed by Harada & Sakata (1992). After the $K(\lambda)$ correction, the intensities R were evaluated by subtraction of $I_{\rm TDS}$. The average of the evaluated R values over the *Pendellösung* oscillation at θ is normalized to $(1 + \cos 2\theta)/2$ for the perfect and nonabsorbing crystal.

Fig. 2 shows the variation in R obtained from Fig. 1. Distinct changes are noted in the intensity itself and in the beat position as well as the beat amplitude. The rate of increase in intensity is not uniform for the heating time. The rate is low in the early stage of heating, then rapidly rises during the period between 25 and 90 h. It decreases again for heating times over 90 h. With regard to wavelength dependence, the intensities do not increase linearly with λ except for specimen II. The slopes are steeper for shorter wavelengths. For heating times longer than 90 h, the slopes remain flat at wavelengths longer than about 0.4 Å. The increasing ratio of intensity compared to specimen I is dependent on the reflection plane. For the specimen heated for 145 h (specimen VI), the ratio at 0.7 Å rises to about 5.7, 7.1, 8.1 and 8.5 times that for specimen I for the 220, 400, 440 and 800 reflections, respectively. The expansion of the beat spacing becomes greater with heating time. Because the *Pendellösung* beats only relate to the coherent part by (5), one sees that the expansion is a result of the decrease in E. The decrease in E is connected to the decrease of crystal perfection through $\mathbf{u}(\mathbf{r})$ of (1). One observes the decrease in the beat amplitude with increasing heating time and wavelength. According to (5), this results from the decrease in E and the increase in λ.

5. Comparison with the theories

The main difference between the two theories lies in the treatment of the correlation length Γ of the amplitude of the wavefield. First, we compare the present data with those obtained using the Kato (1980*a*,*b*) theory, which has the functional form

$$\Gamma = \eta \Lambda_g / E. \qquad (10)$$

The proportionality constant η is expected to be unity by Kato. Here, three unknown parameters E, τ and η are evaluated by the least-squares method. With the aim of characterizing the fitness, the r factor was defined by

$$r = \sum_{i=1}^{N} |R_{\rm mea}(\lambda_i) - R_{\rm cal}(\lambda_i)| \times \left[\sum_{i=1}^{N} R_{\rm mea}(\lambda_i)\right]^{-1} \times 100\ (\%). \qquad (11)$$

N is the number of different wavelengths λ_i at which the J were measured. $R_{\rm mea}$ is the corrected intensity and $R_{\rm cal}$ is the calculated value. Application of the least-squares method yields the fitting parameters and r factors shown in Table 2. The r factors remain less than 2.4%. The τ values are almost zero within the standard deviations of the errors. The best fitted profiles using the parameters are shown in Fig. 2. As far as the intensity is concerned, a good fit is obtained; however, the theoretical positions of the beats deviate gradually from the measurements with increasing heating time. In contrast to Kato's proposal, the best fitted η values differ from unity and range between 0 and 0.041. This means that Kato's original assumption for Γ is inadequate. As mentioned before,

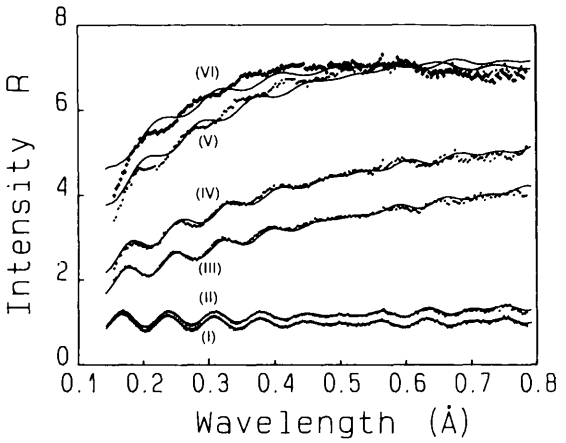

Fig. 2. Intensity R after a correction of $K(\lambda)$ for Fig. 1 and comparison with Kato's theory where Γ is assumed to be $\eta\Lambda_g/E$. Dots and crosses represent the experimental data. Solid lines show the calculated intensities. The fitting parameters of E, τ and η are shown in Table 2. The extinction distance varies from 67 μm at 0.15 Å to 13 μm at 0.78 Å for the σ state of X-ray polarization. The numbers in parentheses are the specimen numbers. Heating times are the same as for Fig. 1.

Table 2. *Results from fitting the theoretical integrated intensities according to Kato, to Becker & Al Haddad and to the present model to the experimental intensity R for the* 400 *reflection*

E is the static Debye-Waller factor and τ is the correlation length of phase factor. The correlation length of wavefield amplitudes by the three different approaches is $\eta\Lambda_g/E$ defined in (10) for Kato, $\tau_2 = \tau/2$ for Becker & Al Haddad and Γ for the present model. The reliability factor r is defined by (11). The r factor for specimen I with $E = 1$ is 1.3%.

	Kato (1980*a*,*b*)				Becker & Al Haddad (1992)			Present model			
Specimen	E	τ (μm)	η	r (%)	E	τ (μm)	r (%)	E	τ (μm)	Γ (μm)	r (%)
II	0.9975 (14)	0.0001 (53)	0.0001 (8)	1.5	0.9977 (1)	0.019 (346)	1.4	0.9974 (2)	0.059 (117)	0.068 (82)	1.2
III	0.9756 (7)	0.0001 (79)	0.0088 (7)	1.3	0.9711 (4)	0.125 (56)	7.7	0.9611 (3)	0.092 (10)	0.179 (9)	1.0
IV	0.9302 (10)	0.0001 (59)	0.0131 (6)	1.5	0.9612 (20)	0.024 (311)	10.2	0.9427 (3)	0.059 (6)	0.190 (6)	0.9
V	0.8326 (31)	0.0001 (58)	0.0252 (10)	2.3	0.8789 (39)	4.24 (15)	7.4	0.8832 (6)	0.053 (5)	0.314 (6)	1.0
VI	0.7558 (44)	0.0001 (42)	0.0411 (12)	2.4	0.8498 (28)	3.39 (7)	5.9	0.8529 (6)	0.082 (3)	0.499 (6)	0.9

the E parameter determines the positions of the beats. Accordingly, E was fixed at the value that satisfies the experimental beat positions, then τ and η were evaluated by the least-squares method. The attempt resulted in poorer agreement.

The same data were compared using the theory of Becker & Al Haddad (1992). Following their procedure, the comparison was made by assuming $\tau_2 = \tau/2$. The fitting parameters and r factors are shown in Table 2. The resultant profiles are drawn in Fig. 3. The theory holds for the data of specimen II with $r = 1.4\%$. The other specimens, however, show large discrepancies in comparison with the previous approach.

We have proposed a model (Takama, Harima & Sato, 1990) assuming that Γ in the Kato theory is free from the extinction distance. It was assumed that Γ is independent of wavelength and varies with crystal perfection and reflection plane. We apply the model to the data. The least-squares method gives the parameters and r factors for the 400 reflection as listed in Table 2. The model gives excellent fits, shown in Fig. 4, and smaller r factors than the other theories. The r factors for the other reflections are also smaller, except for two cases of the 800 reflection in which the Kato approach using η results in $r = 1.6\%$ for specimen IV and $r = 1.8\%$ for specimen VI, where the present model yields 1.8 and 2.9%, respectively. For each reflection of specimen II, the present model actually provides two different sets of the fitting parameters that give almost the same magnitude of r factor. The values of τ and Γ in one set are zero or very nearly zero for each reflection, although E is close to that of the other set. The set that is not listed in Table 2 for the 400 reflection is $E = 0.9975$ (2), $\tau = 0$ (0.029) μm and $\Gamma = 0.022$ (220) μm with $r = 1.2\%$. For the 220 reflection, one set shows that $E = 0.9989$ (1), $\tau = 0.225$ (45) μm and $\Gamma = 0.158$ (57) μm and the other gives $E = 0.9989$ (2), $\tau = 0$ (0.007) μm and $\Gamma = 0$ (0.012) μm with the same r factor of 1.2%. We choose the set with the larger τ and Γ for specimen II for a reason given in § 6. We summarize and display E, τ and Γ in Figs. 5, 6 and 7, respectively. Fig. 8 shows the fitting profiles for the 800 reflection. Specimens with shorter heating times show good fits but poor agreement is obtained for specimens V and VI.

6. Discussion

The statistical dynamical theories of Kato (1980*a*,*b*) and Becker & Al Haddad (1992) have been tested by com-

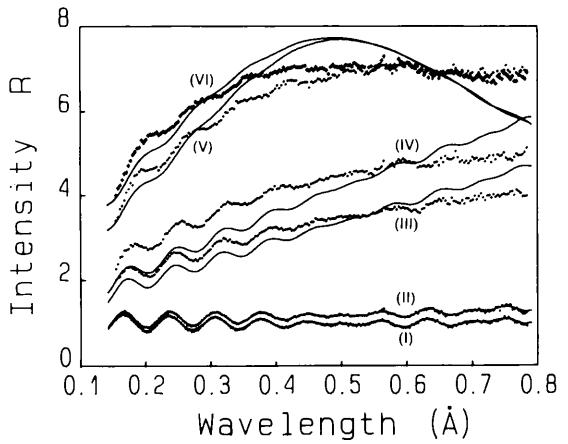

Fig. 3. Fit of Becker & Al Haddad's theory to the experimental data for the 400 reflection with the assumption that $\tau_2 = \tau/2$. Fitting parameters E and τ are shown in Table 2. Specimen numbers appear in parentheses.

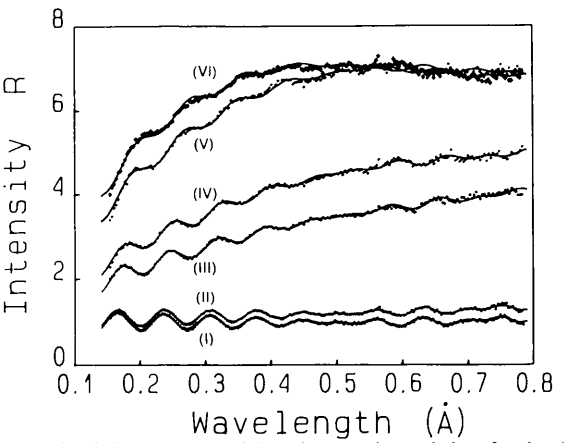

Fig. 4. Fit of the present model to the experimental data for the 400 reflection. Fitting parameters E, τ and Γ are shown in Table 2. Specimen numbers appear in parentheses.

paring measured integrated intensities on a wavelength scale. The present model, in which the Γ in Kato's original theory is replaced by a constant length for a given reflection of a given crystal was also tested with the data. In the two theories, the agreements were judged to be unsatisfactory but a slight modification of Γ in Kato's theory was shown to give better fits.

Kato's original theory did not support the measurements. We introduced the new free parameter η defined by (10) and tried to compare the theory with the data. The treatment showed a fairly good agreement; however, the difference in the beat positions grew with heating as shown in Fig. 2. In addition, the η obtained was of the order of 10^{-2} in most cases. This indicates that Kato's original assumption for Γ is incorrect. The theory of Becker & Al Haddad only agreed with the data from specimen II. For the other specimens, the test showed poorer agreement as shown by Fig. 3 and the r factors in Table 2. The present model provided the best fit of the three approaches.

Schneider *et al.* (1992) made measurements of the integrated reflection power with γ-radiation for CZ silicon heated at 1043 K for 70 h as well as at 1023 K for 24 to 216 h. They observed *Pendellösung* fringes on the thickness scale for the specimen heated at 1043 K. The measurement was described well by the theory of Becker & Al Haddad with small τ of 0.3 μm. They applied the present model to the same data and obtained a good fit with the same magnitude of the r factor for τ = 1 μm and Γ = 0.5 μm. On the other hand, the fringes for the specimens heated at 1023 K were not observed clearly. Accordingly, they averaged the reflection power over the *Pendellösung* oscillations and approximated the thickness dependence of the power by a straight line. The line fitted well to the asymptotic equation equivalent to (7) assuming $\tau_2 = \tau/2$. This implies that

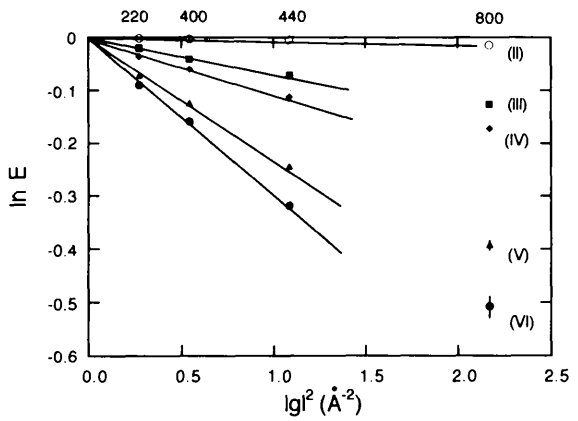

Fig. 5. Natural logarithm of the static Debye-Waller factor E obtained with the present model as a function of g^2. For values without error bars, the standard deviations of the errors are included in the symbols. The mean square displacements obtained from the slopes are listed in Table 1.

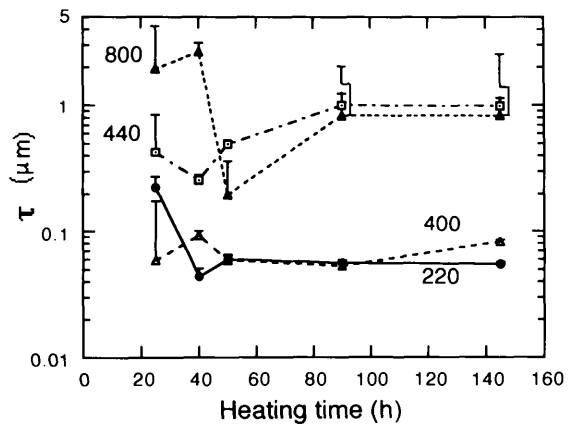

Fig. 6. The correlation length τ of the phase factor for the best fit of the present model to the data as a function of heating time. The error bars are shown for the upper part only to avoid complexity.

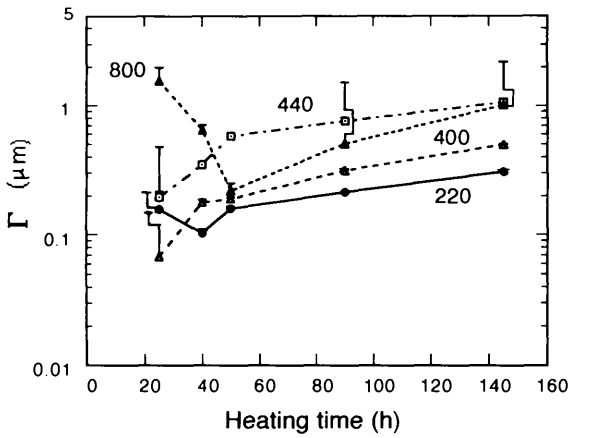

Fig. 7. The correlation length Γ of wavefield amplitudes for the best fit of the present model to the data as a function of heating time. The error bars are shown for the upper part only to avoid complexity.

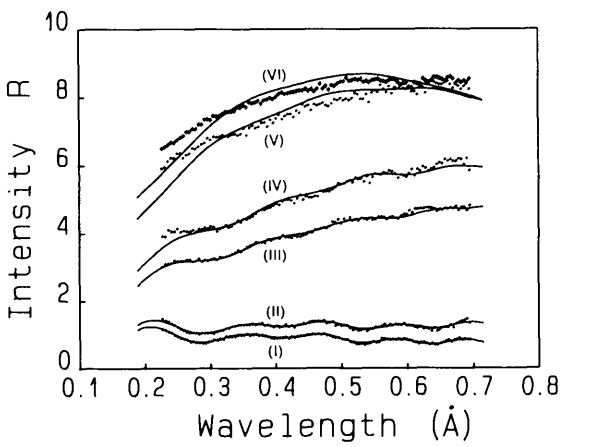

Fig. 8. Comparison of R for the 800 reflection with the present model. Dots and crosses show experimental data. Solid lines show calculated values. The fitting parameters E, τ and Γ are shown in Table 2. Specimen numbers appear in parentheses.

the imperfection of the crystals is characterized by E alone. The basic characteristic of their experiments is that R shows a linear dependence on the thickness. In the present experiments, the linear increase of R with λ in specimen II was the exception. The profiles were explained by the two different sets of parameters. One set was essentially the same result as from (7). In contrast to the work of Schneider *et al.* (1992), τ and Γ were required to describe the profiles for the other specimens. The present specimens were heated at 1223 K whereas those of Schneider *et al.* (1992) were heated at 1023 and 1043 K. The temperature difference influences the form of the induced defects as mentioned in § 3. Therefore, the strain fields in the two experiments are thought to differ from each other, especially for longer heating times. The nature of the strain field may be responsible for the difference in R between the two investigations. It should be noted that the present model shows greater flexibility in describing diffraction from crystals with a variety of imperfections.

The amplitude correlation length Γ obtained by the present model was concentrated between 0.07 and 1.6 μm as displayed in Fig 7. It seems to increase slightly with the heating time and the index of the reflection plane. The present experiment covers the extinction distance Λ_g for the σ polarization from 11 μm at $\lambda = 0.79$ Å for the 220 reflection to 96 μm at 0.225 Å for the 800 reflection. The Γ obtained was about 1% of the extinction distance.

The τ of best fit are represented in Fig. 6. They exist between 0.04 and 2.6 μm. The length of τ shows a tendency to remain almost constant for a reflection. The length can be roughly estimated by the volume of the precipitate. According to Voronkov, Piskunov, Chukhovskii & Maksimov (1987), τ is given by the relation of $\tau \simeq 2r_o$, where r_o is the radius of a spherical defect. The volume of the precipitate introduced by heating in argon gas has been measured by transmission electron microscopy (Wada, Inoue & Kohra, 1980). The volume after heating at 1223 K for 25 h is about 1.3×10^9 Å^3, as obtained from Fig. 2 in their paper. They observed precipitates in the form of square-shaped platelets. Thus, if we assume a spherical precipitate, the mean radius r_o is about 0.07 μm. It gives rise to a τ of 0.14 μm, which is compatible with the present results. This is the reason why we chose the set of fitting parameters with larger values of τ and Γ for specimen II in the previous section.

Fig. 5 represents the natural logarithm of E as a function of g^2. Except for the 800 reflection, the dependence of $\ln E$ on g^2 can be approximated by straight lines. If the distribution of $u(r)$ is Gaussian, or if the mean square displacement $\langle u^2 \rangle$ is small,

$$E = \exp\left[-\left(2\pi^2/3\right)g^2\langle u^2\rangle\right] = \exp\left(-2\pi^2 g^2\langle \xi^2\rangle\right), \quad (12)$$

where $\langle \xi^2 \rangle$ is the mean square displacement of a lattice point in the direction of the vector $\mathbf{g}$. From the slope of the line, $\langle u^2 \rangle = 3\langle \xi^2 \rangle$ can be derived. The values for $\langle u^2 \rangle$ are listed in Table 1. In accurate measurements of the structure factors, Saka & Kato (1986) derived the thermal Debye-Waller factor β_t of silicon at 293 K. The symmetric part of the Debye-Waller factor is given by $\exp[-\beta_t(h^2 + k^2 + l^2)]$ with $\beta_t = 3.877 \times 10^{-3}$. This leads to $\langle u^2 \rangle$ of 0.01738 Å^2. The static displacement caused by 50 h heating has almost the same magnitude as the thermal vibration.

It is of interest to see how much each component contributes to the total intensity. Fig. 9 shows an example of the 220 reflection from specimen V. The incoherent component plays the main role in the increase in R. The coherent component remains almost unchanged with λ whereas the mixed component gradually increases. The decrease in the incoherent component at long wavelengths is offset by the increased mixed component. Thus, the total intensity does not show the λ dependence at long wavelengths.

In the statistical dynamical theory, X-ray waves are assumed to travel along the directions of the incident and the diffracted beams. Consequently, diffuse scattering going out of the Borrmann fan is not expected. As seen in Fig. 8 for the 800 reflection, the fit of the present model becomes slightly worse with increasing heating time. This might be caused by neglection of the diffuse scattering that increases with the order of reflection. Recently, Kato (1991) has proposed a more rigorous theory that is based on fundamental equations with a higher degree of approximation than the Takagi-Taupin equations. It is expected that the theory will overcome the discrepancy in the future.

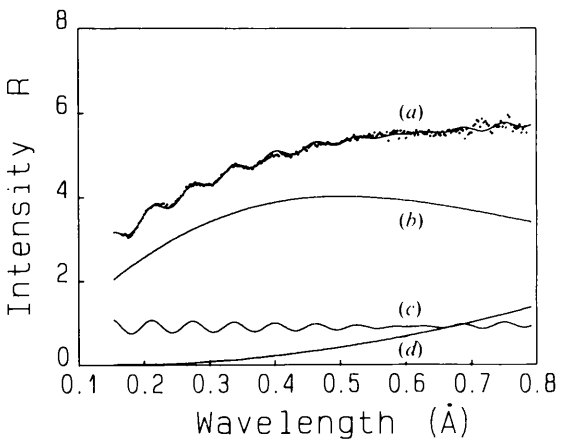

Fig. 9. The total intensity and its three components obtained by the present model for reflection 220 and specimen V (90 h heating at 1223 K). (*a*) Total intensity, sum of (*b*) the incoherent component, (*c*) the coherent component and (*d*) the mixed component. The coherent component contains the Borrmann term. The fitting parameters are $E = 0.9320$ (4), $\tau = 0.056$ (3) μm and $\Gamma = 0.214$ (4) μm with r factor 1.0%.

The authors acknowledge the valuable advice of Professor N. Kato of Meijoh University on this work. They thank Professors J. Harada and M. Sakata of Nagoya University who allowed the use of their program for calculating the thermal diffuse scattering. They also acknowledge Dr T. Abe of the Shin-Etsu Semiconductor Company for kindly supplying silicon wafers. They are indebted to Mr T. Little of the University of Illinois for a critical reading of the manuscript. This work was supported by a Grant in Aid of Scientific Research (no. 01580049, TT) from the Ministry of Education, Science and Culture of Japan to which the authors' thanks are due.

References

AL HADDAD, M. & BECKER, P. J. (1988). *Acta Cryst.* A**44**, 262-270.
BECKER, P. & AL HADDAD, M. (1990). *Acta Cryst.* A**46**, 123-129.
BECKER, P. & AL HADDAD, M. (1992). *Acta Cryst.* A**48**, 121-134.
BURAS, B. & GERWARD, L. (1975). *Acta Cryst.* A**31**, 372-374.
DARWIN, C. G. (1922). *Philos. Mag.* **43**, 800-829.
GRAF, H. A., SCHNEIDER, J. R., FREUND, A. K. & LEHMANN, M. S. (1981). *Acta Cryst.* A**37**, 863-871.
GUIGAY, J. P. (1989). *Acta Cryst.* A**45**, 241-244.
HAMILTON, W. C. (1957). *Acta Cryst.* **10**, 629-634.
HARADA, J. & SAKATA, M. (1992). Personal communication.
KATO, N. (1980*a*). *Acta Cryst.* A**36**, 763-769.
KATO, N. (1980*b*). *Acta Cryst.* A**36**, 770-778.
KATO, N. (1991). *Acta Cryst.* A**47**, 1-11.
OLEKHNOVICH, N. M., KARPEI, A. L., OLEKHNOVICH, A. I. & PUZENKOVA, L. D. (1983). *Acta Cryst.* A**39**, 116-122.
SAKA, T. & KATO, N. (1986). *Acta Cryst.* A**42**, 469-478.
SASAKI, S. (1989). KEK Report, Vol. 88-14, pp. 1-36. Photon Factory, Ibaraki, Japan.
SCHNEIDER, J. R., BOUCHARD, R., GRAF, H. A. & NAGASAWA, H. (1992). *Acta Cryst.* A**48**, 804-819.
SHIMURA, F. (1989). *Semiconductor Silicon Crystal Technology*. San Diego: Academic Press.
TAKAGI, S. (1962). *Acta Cryst.* **15**, 1311-1312.
TAKAMA, T., HARIMA, H. & SATO, S. (1990). *Acta Cryst.* A**46**, C412.
TAKAMA, T., IWASAKI, M. & SATO, S. (1980). *Acta Cryst.* A**36**, 1025-1030.
TAKAMA, T. & SATO, S. (1988). *Aust. J. Phys.* **41**, 433-448.
TAUPIN, D. (1964). *Bull. Soc. Fr. Mineral. Cristallogr.* **87**, 469-511.
VORONKOV, S. N., PISKUNOV, D. I., CHUKHOVSKII, F. N. & MAKSIMOV, S. K. (1987). *Sov. Phys. JETP*, **65**, 624-629.
WADA, K., INOUE, N. & KOHRA, K. (1980). *J. Cryst. Growth*, **49**, 749-752.
ZACHARIASEN, W. H. (1967). *Acta Cryst.* **23**, 558-564.

Acta Cryst. (1994). A**50**, 246–252

The Multiple-Diffraction Effect in Accurate Structure-Factor Measurements of PtP_2 Crystals

BY KIYOAKI TANAKA*

Chemistry Department, Nagoya Institute of Technology, Gokiso-machi Showa-ku, Nagoya 466, *Japan*

SHINJI KUMAZAWA, MICHIAKI TSUBOKAWA AND SIGEO MARUNO

Department of Electrical and Computer Engineering, Nagoya Institute of Technology, Gokiso-machi Showa-ku, Nagoya 466, *Japan*

AND ICHIMIN SHIROTANI

Department of Electrical Engineering, Muroran Institute of Technology, Mizumoto-cho 27-1, *Hokkaido* 050, *Japan*

(*Received* 26 *April* 1993; *accepted* 18 *August* 1993)

Abstract

Accurate X-ray intensities of a PtP_2 crystal were measured with the multiple-diffraction effect avoided by using the ψ rotation of the crystal around the scattering vector. The results were compared with those of a measurement made without avoiding the effect. The extinction parameters were more isotropic and the peaks of the deformation density were significantly smaller when multiple diffraction was avoided. In the measurement made without avoiding the effect, the number of structure factors affected by more than 1% was 403 from 936 reflections measured. Of 272 strong reflections with $\sin\theta/\lambda < 0.6$ Å^{-1} and $F_{obs} > 200$, 27 reflections were affected by more than 1%. These facts, as well as the smaller R values, indicate that the multiple-diffraction effect cannot be neglected in electron-density studies of crystals including heavy atoms. To assess the intensity fluctuation calculated in the present study, the intensities of 200 reflections were measured at intervals of 0.5° from 0 to 180° in ψ and compared with the calculated values. The variations of the measured and calculated intensities with ψ correspond to each other, which indicates that the present method can

* To whom correspondence should be addressed.